Available online at www.sciencedirect.com
SCIENCE DIRECT®
Solid-State Electronics 47 (2003) 2289–2294
SOLID-STATE ELECTRONICS
www.elsevier.com/locate/sse

ICP dry etching of ZnO and effects of hydrogen

K. Ip [a,*], M.E. Overberg [a], K.W. Baik [a], R.G. Wilson [b], S.O. Kucheyev [c,1], J.S. Williams [c], C. Jagadish [c], F. Ren [d], Y.W. Heo [a], D.P. Norton [a], J.M. Zavada [e], S.J. Pearton [a]

[a] *Department of Materials Science and Engineering, University of Florida, Gainesville, FL 32611, USA*
[b] *Consultant, Stevenson Ranch, CA 91381, USA*
[c] *Department of Electronic Materials Engineering, Australian National University, Canberra ACT 0200, Australia*
[d] *Department of Chemical Engineering, University of Florida, Gainesville, FL 32611, USA*
[e] *US Army Research Office, Research Triangle Park, NC 27709, USA*

Received 27 July 2002; received in revised form 2 November 2002; accepted 17 December 2002

Abstract

Two different plasma chemistries for etching ZnO were examined. Both Cl_2/Ar and CH_4/H_2/Ar produced etch rates which increased linearly with rf power, reaching values of ~1200 Å/min for Cl_2/Ar and ~3000 Å/min for CH_4/H_2/Ar. The evolution of surface morphology, surface composition, and PL intensity as a function of energy during etching were monitored. The effect of H in ZnO was studied using direct implantation at doses of 10^{15}–10^{16} cm^{-2}, followed by annealing at 500–700 °C. The hydrogen shows significant outdiffusion at 500 °C and is below the detection limits of SIMS after 700 °C anneals. SEM of the etched features showed anisotropic sidewalls, indicative of an ion-driven etch mechanism.

1. Introduction

ZnO is attracting attention for use in UV opto-electronics, gas sensing, surface acoustic wave devices, varistors, piezoelectric transducers, micro-actuators, and transparent electrodes [1–23]. It is available in bulk, cleavable substrate form and recently p-type doping has been achieved which opens up a range of additional device possibilities. The development of high resolution etch processes is necessary for any device fabrication schemes in ZnO. Wet chemical etching of ZnO has been reported with a number of acid solutions, including HCl, HNO_3, and NH_4Cl [24–26]. However, wet etch processes are generally isotropic with limited resolution and poor selectivity. Very few reports have appeared on dry etching of ZnO [27,28], especially with the type of high-density plasma sources favored in modern manufacturing environments because of their versatility and excellent uniformity.

In this paper we report an investigation of inductively coupled plasma (ICP) etching of bulk ZnO in two different plasma chemistries (CH_4/H_2/Ar and Cl_2/Ar) as a function of the incident ion energy. The role of hydrogen was further investigated by direct implantation of hydrogen and measurements of its effects in the luminescence and structural properties. Hydrogen is predicted to be a shallow donor in ZnO and some indirect measurements are consistent with this theory [29–39].

2. Experimental

Bulk, wurtzite(0 0 0 1) ZnO crystals obtained from Eagle–Picher were used for all experiments. The samples were nominally undoped ($n \sim 8 \times 10^{16}$ cm^{-3}) and the

* Corresponding author. Fax: +1-352-846-1182.
[1] Present address: Lawrence Livermore National Laboratory, Livermore, CA, USA.

0038-1101/$ - see front matter © 2003 Elsevier Ltd. All rights reserved.
doi:10.1016/S0038-1101(03)00211-9

Zn-terminated surface was the one used in all cases. Etching was performed in a Unaxis 790 reactor, which employs a 2 MHz ICP source and 13.56 MHz rf-biased cathode. Electronic grade gases were introduced through mass flow controllers at a total flow rate of 15–16 standard cubic centimeters per minute. The two gas mixtures investigated were $3CH_4/8H_2/5Ar$ and $10Cl_2/5Ar$. The ICP source power was held constant at 500 W and the process pressure at 1 mTorr. The ion energy was varied by changing the rf chuck power from 50 to 300 W, producing dc self-biases in the range of −75 to −344 V for Cl_2/Ar and −91 to −294 V for $CH_4/H_2/Ar$. Etch rates were measured using stylus profilometer, while the optical quality was obtained from room temperature photoluminescence measurements using a He–Cd laser excitation. The surface morphology was examined using tapping mode atomic force microscopy (AFM) measurements and scanning electron microscopy (SEM), while the near-surface stoichiometry was measured by Auger electron microscopy (AES). To further examine the role of hydrogen in ZnO, direct implantation of 100 keV $^1H^+$ or $^2H^+$ at doses of 10^{15}–10^{16} cm^{-2} was also performed, followed by either secondary ion mass spectrometry (SIMS) or Rutherford backscattering/channeling (RBS/C).

3. Results and discussion

Fig. 1 shows the ZnO etch rates in both chemistries as a function of rf chuck power. The $CH_4/H_2/Ar$ produces higher rates as expected from an examination of the probable Zn etch products, namely $(CH_3)_3Zn$, which has a vapor pressure of ~300 Torr at 20 °C compared to $ZnCl_2$ which has a vapor pressure of 1 Torr at 428 °C.

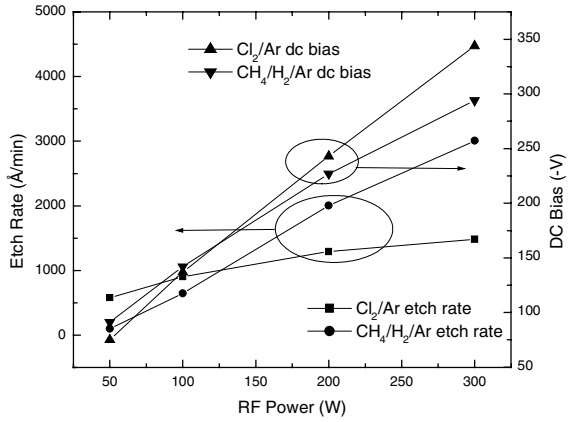

Fig. 1. Etch rates of ZnO as a function of rf chuck power in ICP $CH_4/H_2/Ar$ or Cl_2/Ar discharges. The dc self-bias on the cathode is also shown.

The etch product for oxygen is most likely O_2, although OH may play a role in the $CH_4/H_2/Ar$ chemistry. For ion-driven etch processes, the etch rate is generally proportional to $E^{0.5} - E_{TH}^{0.5}$, where E is the average energy of incident ions and E_{TH} is the threshold for initiating etching [40]. The ion energy can be obtained from the dc self-bias by adding the plasma potential (25 V in our system). This analysis produces a value for E_{TH} of ~96 eV for the $CH_4/H_2/Ar$ chemistry.

Lee et al. [15] reported that reactively sputtered ZnO epitaxial films grown on sapphire showed a major increase in band-edge emission after exposure to a H_2 plasma, while the deep level emission was largely quenched. Fig. 2 shows PL spectra before and after ICP etching of different rf chuck powers. There is a decrease of approximately a factor of 4 even for the low bias condition, which shows that ZnO is susceptible to ion-induced damage during plasma etching. In etching real

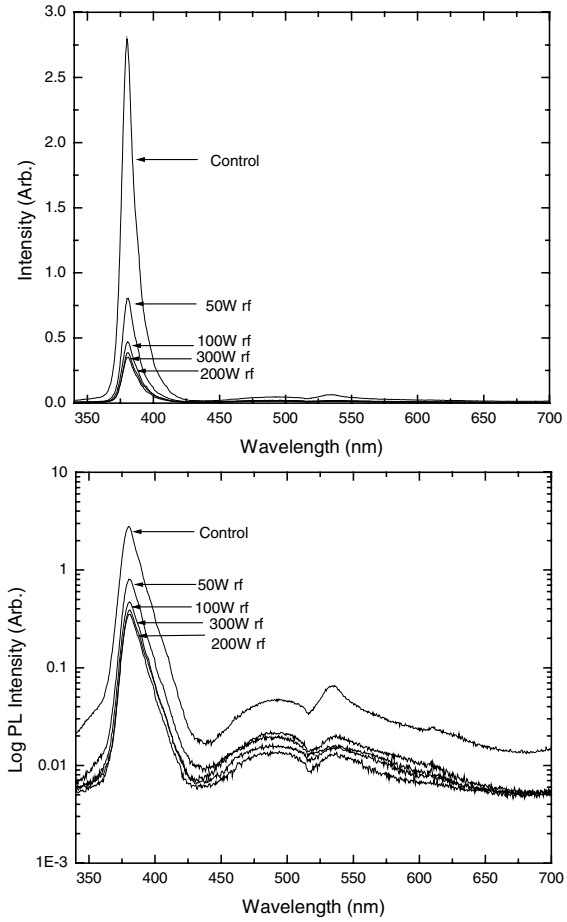

Fig. 2. Room temperature PL spectra from ZnO etched in ICP $CH_4/H_2/Ar$ discharges at different rf chuck powers. The spectra are shown on both log (top) and linear (bottom) scales.

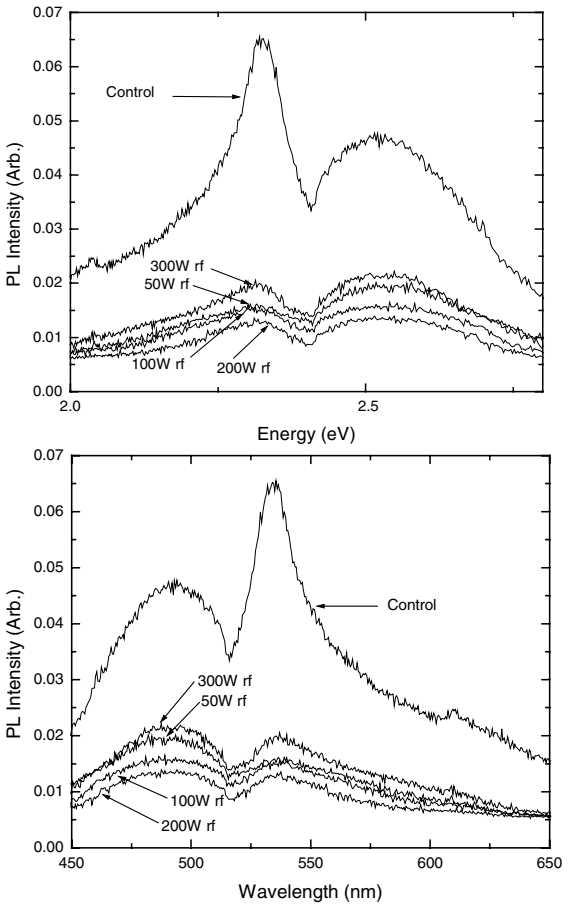

Fig. 3. Room temperature, deep-level PL emission from ZnO etched in ICP $CH_4/H_2/Ar$ discharges at different rf chuck powers. The data are shown on both energy (top) and wavelength (bottom) scales.

device structures it would be necessary to minimize both ion energy and ion flux toward the end of the process in order to minimize lattice damage. Fig. 3 shows a close-up of the deep level emission spectra—the intensity of these transitions is also decreased by the etch process. At this stage, it is not clear if this is a result of hydrogen incorporation, or simply a decrease in overall intensity because of the introduction of non-radiative centers.

Fig. 4 shows AFM surface scans taken before and after etching with $CH_4/H_2/Ar$ at different rf chuck powers. The surface morphology is clearly dependent on the incident ion energy, and most likely results from differences in the removal rates of Zn and O etch products. Fig. 5 shows the root-mean-square (RMS) roughness measured over 5×5 μm^2 areas, as a function of the rf chuck power. The roughness goes through a minimum at 200 W rf power, corresponding to an ion energy of ~251 eV. At this incident ion energy, the surface roughness is the same as for the unetched control material. Under these conditions the etch rate is ~2000 Å/min, which is a practical value for most device processing applications.

A smooth surface morphology is a good indicator of equi-rate removal of both Zn and O during etching. Fig. 6 shows AES surface scans before and after ICP $CH_4/H_2/Ar$ etching at 200 W rf power. Approximately 60 Å of ZnO was removed by Ar ion sputtering in the AES analysis chamber prior to analysis to remove adventitious carbon and other atmospheric contaminants. The Zn-to-O ratio is identical within experimental error and demonstrates that $CH_4/H_2/Ar$ etching is capable of maintaining the surface stoichiometry of ZnO through equi-rate removal of the Zn and O etch products.

Given our results showing that $CH_4/H_2/Ar$ has an ion-driven etch mechanism for ZnO and can maintain smooth, stoichiometric surfaces, we would expect to see highly anisotropic pattern transfer using this plasma chemistry. Fig. 7 shows features produced with an optimized $CH_4/H_2/Ar$ process and photoresist masking. The sidewall striations are due to initial resist sidewall roughness, but one can see excellent high fidelity pattern transfer into the ZnO.

Since atomic hydrogen is predicted to have interesting effects on both the electrical and optical properties of ZnO, we examined its behavior in more detail. Fig. 8 shows SIMS profiles of implanted ^2H as a function of subsequent annealing temperature. A significant evolution of deuterium out of the ZnO occurs at temperatures as low as 500 °C, with the remaining deuterium decorating residual implant damage. Only 0.2% of the original dose remains in the sample after 600 °C annealing, and the signal is below the SIMS detection limit of 3×10^{15} cm^{-3} after 700 °C annealing. The stability of ^2H retention in ZnO is significantly lower than in GaN, where temperatures of ~900 °C were required to remove all of the deuterium in samples implanted under comparable conditions to those employed here [41].

The ^2H implantation caused a complete loss of band-edge luminescence, with only a partial (10%) recovery after 700 °C annealing. By sharp contrast, only a minor increase in RBS/C yield was observed for ^1H implant doses an order of magnitude higher than used for the SIMS and luminescence experiments. Fig. 9 shows that ^1H implantation of a dose of 10^{16} cm^{-2} (100 keV) did not affect the measurable backscattering yield near the sample surface, but did result in a small ion scattering peak in the region where the nuclear energy ion profile of 100 keV H^+ ions is a maximum (at around 7000 A). The yield at this depth was ~7.8% after implantation, compared to ~6.5% of the random level prior to implantation. All of this data indicates that local defects created by the implantation control the optical properties of the ZnO, even after 700 °C annealing.

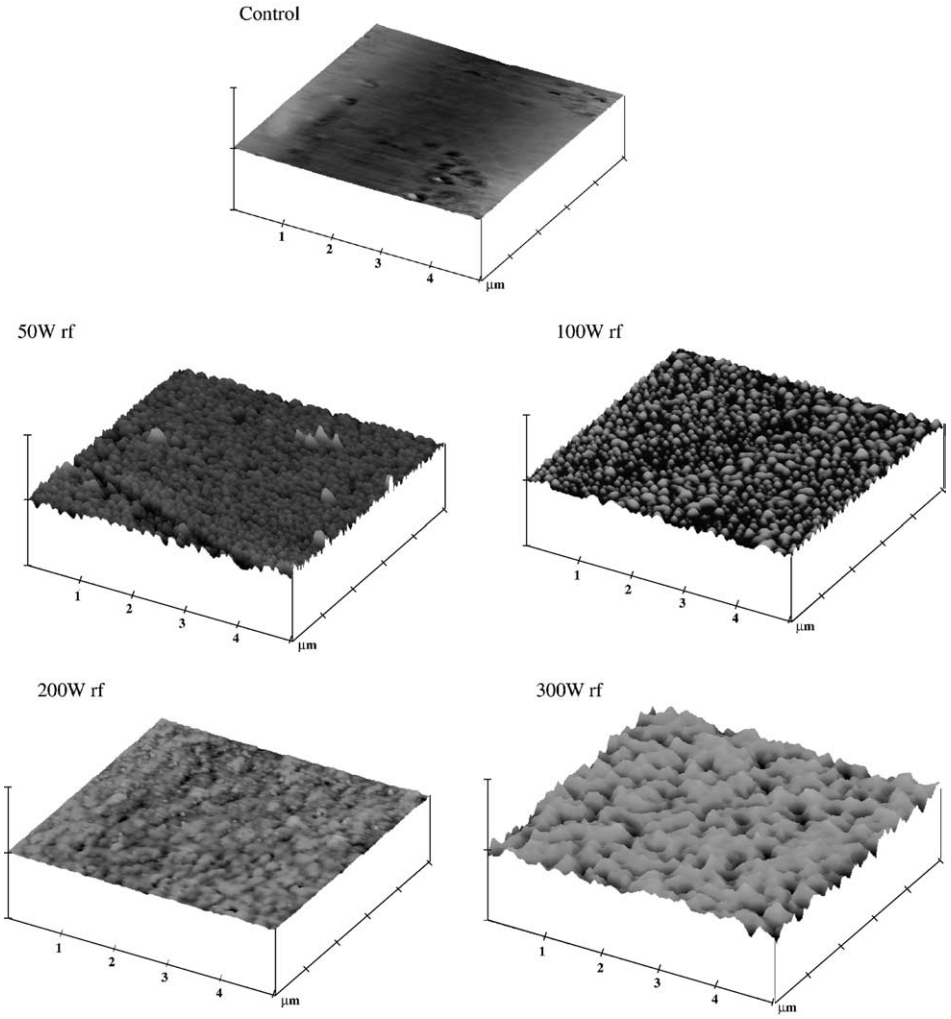

Fig. 4. AFM scans of ZnO before and after ICP $CH_4/H_2/Ar$ etching at different rf chuck powers. The z-scale is 150 nm/div.

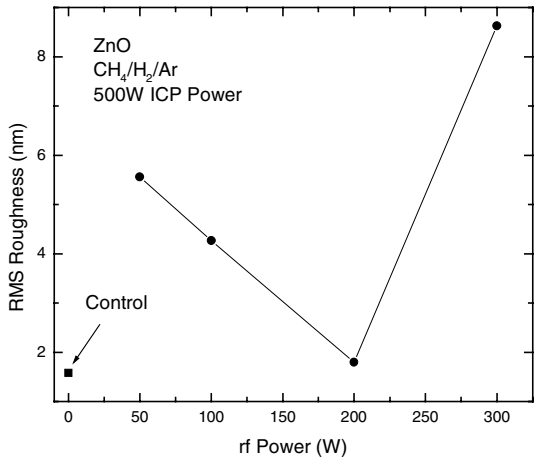

Fig. 5. RMS roughness of ZnO surfaces etched in ICP $CH_4/H_2/Ar$ discharges at different rf chuck powers.

4. Summary and conclusions

Smooth, anisotropic pattern transfer in ZnO can be achieved with ICP $CH_4/H_2/Ar$ discharges render optimum conditions. The etched surface is smooth and stoichiometric under these conditions and the etching proceeds by an ion-driven mechanism with a threshold ion energy of ~96 eV. ICP Cl_2/Ar discharges also produce practical etch rates for ZnO but are slower than with $CH_4/H_2/Ar$ because of the low volatility of the $ZnCl_2$ etch product. The luminescence intensity from the ZnO is significantly degraded by the dry etching and indicates that hydrogen is not being incorporated into the near-surface region at concentrations high enough to remove the non-radiative defects created. Direct implantation of deuterium was used to examine the thermal stability of hydrogen retention and 700 °C anneals

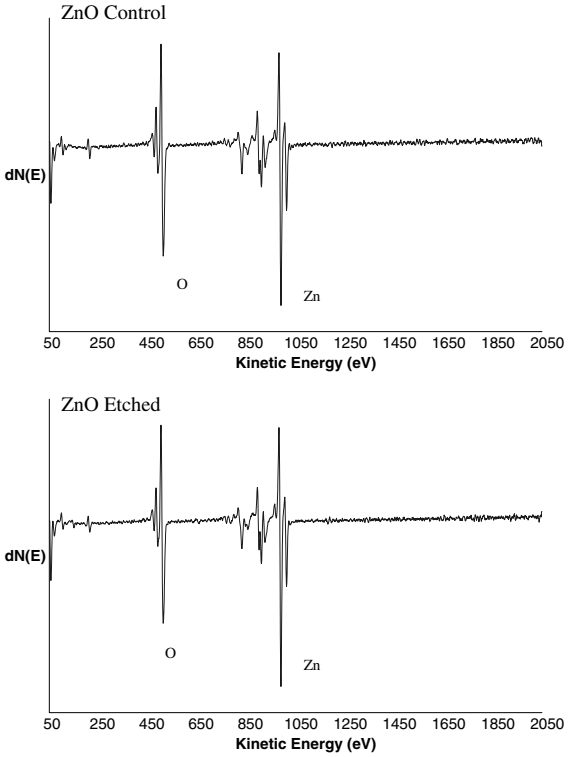

Fig. 6. AES surface scans before (top) and after (bottom) etching in ICP $CH_4/H_2/Ar$ discharges. The spectra were taken at a depth of ~60 Å by first sputtering briefly with an Ar^+ beam.

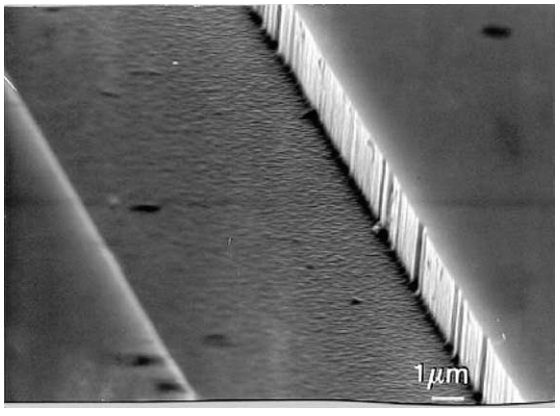

Fig. 7. SEM micrograph of features etched into ZnO using an ICP $CH_4/H_2/Ar$ discharge. The photoresist mask has been removed.

removed the deuterium to below the detection sensitivity of SIMS.

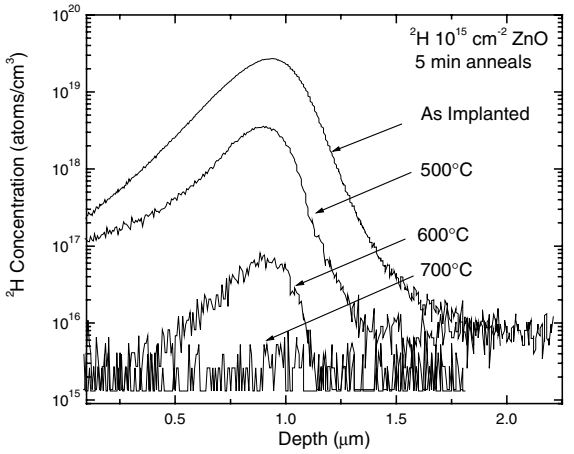

Fig. 8. SIMS profiles of implanted ^2H in ZnO as a function of annealing temperature.

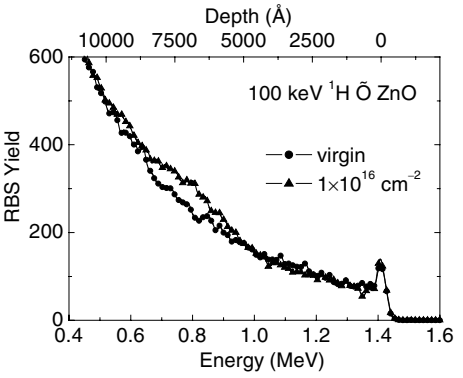

Fig. 9. RBS/C spectra from ZnO before and after implantation with 100 keV $^1H^+$ ions at a dose of 10^{16} cm^{-2}.

Acknowledgements

The work at UF is partially supported by ARO and NSF (DMR0101438 and CTS 991173).

References

[1] Look DC. Mater Sci Eng B 2001;80:383.
[2] Ohta H, Kawamura K, Orita M, Hirano M, Sarukura N, Hosono H. Appl Phys Lett 2000;77:475.
[3] Joseph M, Tabata H, Kawai T. Jpn J Appl Phys 1999; 38:L1205.
[4] Krishnamoorthy S, Iliadis AA, Inumpudi A, Choopun S, Vispute RD, Venkatesan T. Solid-State Electron 2002; 46:1631.
[5] Zu P, Tang ZK, Wong GKL, Kawasaki M, Ohtomo A, Koinuma K, et al. Solid-State Commun 1997;103:459.

[6] Bagnall DM, Chen YR, Zhu Z, Yao T, Koyama S, Shen MY, et al. Appl Phys Lett 1997;70:2230.
[7] Liang S, Gorla CR, Emanetoglu NW, Liu Y, Mayo WE, Lu Y. J Electron Mater 1998;27:L72.
[8] Liang S, Sheng H, Liu Y, Huo Z, Lu Y, Shen H. J Cryst Growth 2001;225:110.
[9] Wraback M, Shen H, Liang S, Gorla CR, Lu Y. Appl Phys Lett 1999;76:507.
[10] Aoki T, Look DC, Hatanaka Y. Appl Phys Lett 2000;76:3257.
[11] Chang CC, Chen YE. IEEE Trans Ultrason Ferroelectrics Freq Control 1997;44:624.
[12] Verghese PM, Clarke DR. J Appl Phys 2000;87:4330.
[13] Gorla CR, Emanetoglu NW, Liang S, Mayo WE, Lu Y, Wraback M, et al. J Appl Phys 1999;85:2595.
[14] Wraback M, Shen H, Liang S, Gorla CR, Lu Y. Appl Phys Lett 1999;74:507.
[15] Lee J-M, Kim K-K, Park S-J, Choi W-K. Appl Phys Lett 2001;78:2842.
[16] Nause JE. III–V's Review 1999;12:28.
[17] Chen Y, Bagnell D, Yao T. Mater Sci Eng B 2000;75:190.
[18] Look DC, Reynolds DC, Hemsky JW, Jones RL, Sizelove JR. Appl Phys Lett 1999;75:811.
[19] Look DC, Hemsky JW, Sizelove JR. Phys Rev Lett 1999;82:2552.
[20] Auret FD, Goodman SA, Hayes M, Legodi MJ, van Laarhoven HA, Look DC. Appl Phys Lett 2002;80:956.
[21] Kucheyev SO, Bradley JE, Williams JS, Jagadish C, Swain MV. Appl Phys Lett 2002;80:956.
[22] Reynolds DC, Look DC, Jogai B. Solid-State Commun 1996;99:873.
[23] Clarke DR. J Am Ceram Soc 1999;82:485.
[24] Vellaloop WJ, Visser CCG, Sarro PW, Venana A. Sensors Actuat A 1990;21–23:1027.
[25] Li Y, Tompa GS, Liang S, Gorla C, Lu Y, Doyle J. J Vac Sci Technol A 1997;15:1063.
[26] Gardeniers JGE, Rittersonk ZM, Burger GJ. J Appl Phys 1998;83:7844.
[27] Swanson GD, Tanagawa T, Polla DL. Electrochem Soc Ext Abstr 1990;90–92:1082.
[28] Lee J-M, Chang K-M, Kim K-K, Choi W-K, Park SJ. J Electrochem Soc 2001;148:G1.
[29] van de Walle CC. Phys Rev Lett 2000;85:1012.
[30] van de Walle CC. Phys Stal Solidi B 2002;229:221.
[31] Kilic C, Zunger Z. Appl Phys Lett 2002;81:73.
[32] van de Walle CC. Physica B 2001;308–310:899.
[33] Cox SJF, Davis EA, Cottrell SP, King PJC, Lord JS, Gil JM, et al. Phys Rev Lett 2001;86:2601.
[34] Cox SJF, Davis EA, King PJC, Gil JM, Alberto HV, Vilao RC, et al. J Phys C 2001;13:9001.
[35] Hofmann DM, Hofstaetter A, Leiter F, Zhou H, Henecker F, Meyer BK, et al. Phys Rev Lett 2002;88:045504.
[36] Baik SJ, Jang JH, Lee CH, Cho WY, Lim KS. Appl Phys Lett 1997;70:3516.
[37] Theys B, Sallet V, Jomard F, Lusson A, Rommeluere J-F, Teukam Z. J Appl Phys 2002;91:3922.
[38] Ohashi N, Ishigaki T, Okada N, Sekiguchi T, Sakaguchi I, Haneda H. Appl Phys Lett 2002;80:2869.
[39] Bogatu V, Goldenbaum A, Many A, Goldstein Y. Phys Stal Solidi B 1999;212:89.
[40] Steinbruchel C. Appl Phys Lett 1989;55:1960.
[41] Wilson RG, Pearton SJ, Abernathy CR, Zavada JM. J Vac Sci Technol A 1995;13:719.